Drug Delivery

ISSN: 1071-7544 (Print) 1521-0464 (Online) Journal homepage: informahealthcare.com/journals/idrd20

The effective combination therapy against human osteosarcoma: doxorubicin plus curcumin co-encapsulated lipid-coated polymeric nanoparticulate drug delivery system

Lin Wang, WeiGuo Wang, Ze Rui & DongSheng Zhou

To cite this article: Lin Wang, WeiGuo Wang, Ze Rui & DongSheng Zhou (2016) The effective combination therapy against human osteosarcoma: doxorubicin plus curcumin co-encapsulated lipid-coated polymeric nanoparticulate drug delivery system, Drug Delivery, 23:9, 3200-3208, DOI: 10.3109/10717544.2016.1162875

To link to this article: https://doi.org/10.3109/10717544.2016.1162875

Published online: 17 May 2016.

Drug Delivery

http://informahealthcare.com/drd
ISSN: 1071-7544 (print), 1521-0464 (electronic)

Drug Deliv, 2016; 23(9): 3200–3208
 DOI: 10.3109/10717544.2016.1162875

Taylor & Francis
Taylor & Francis Group

RESEARCH ARTICLE

The effective combination therapy against human osteosarcoma: doxorubicin plus curcumin co-encapsulated lipid-coated polymeric nanoparticulate drug delivery system

Lin Wang[1,2], WeiGuo Wang[3], Ze Rui[2], and DongSheng Zhou[1]

[1]*Department of Orthopaedics, Shandong Provincial Hospital Affiliated to Shandong University, Ji'nan, P.R. China,* [2]*Department of Orthopaedics, Affiliated Hospital of Taishan Medical University, Taian, P.R. China, and* [3]*Department of Orthopaedics, General Hospital of Ji'nan Military Command, Ji'nan, P.R. China*

Abstract

Objective: To overcome both the dose-limiting side effects of conventional chemotherapeutic agents and the therapeutic failure incurred from multidrug resistant (MDR) in osteosarcoma (OS), biodegradable lipid-coated polymeric nanoparticles (LPNs) were explored for the loading of doxorubicin (DOX) and curcumin (CUR).

Methods: DOX plus CUR co-encapsulated LPNs (DOX + CUR LPNs) of mixed lipid monolayer shell and biodegradable polymer core were prepared. The cytotoxicity effect of DOX + CUR LPNs, single drug loaded LPNs, and free drug solutions were evaluated on human OS cell line KHOS cells and mice KHOS cells xenograft *in vivo*.

Results: DOX + CUR LPNs displayed a curative effect on OS cell lines than the free drug counterparts. Also, best anti-OS effects were observed on the animal model compared with other groups tested.

Conclusion: This promising dual drugs co-encapsulated lipid-coated polymeric nanoparticulate drug delivery system enhanced the cell delivery and activity of drugs against human OS cancer cell lines and in cancer bearing mice. This research may offer new options for the treatment of OS.

Keywords

Co-encapsulated, combination therapy, drug delivery system, human osteosarcoma, lipid-coated polymeric nanoparticle

History

Received 7 January 2016
Revised 2 March 2016
Accepted 3 March 2016

Introduction

Osteosarcoma (OS) is the most common primary malignant bone tumor in children and young adults and accounts for 60% of primary bone cancers diagnosed in the first two decades of life (Longhi et al., 2006). Current approved treatments for OS include surgery and chemotherapy (Siegel et al., 2013). The cure rate of patients with localized OS ranges from 15 to 20% with surgery alone, while improves to approximately 70% when combined with chemotherapy (Schwartz et al., 2007). Several classes of chemotherapeutic agents are used in primary and adjuvant treatment for OS. Until now, doxorubicin (DOX), cisplatin and methotrexate are the commonly used chemotherapeutics to treat OS. However, despite advances in surgical techniques and neoadjuvant chemotherapy regimens, the failure of current treatment accounts for about 30%, which is mainly due to drug resistance in patients with stage IV cancer (Desandes, 2007; Li S et al., 2015).

Multidrug resistance (MDR) in OS therapy due to various mechanisms, including decreased intracellular drug accumulation mediated by P-glycoprotein (P-gp), apoptosis inhibition by Bcl-2 or p53 or miRNAs, up-regulation of nuclear factor kappa B (NF-κB) activity, blocking the binding of chemotherapy drugs DNA Topo II, detoxification in the cell by GSTP1, enhanced DNA repair by ERCC or APE1 and cancer stem cells mediated resistance (Nedelcu et al., 2008; Rajkumar & Yamuna, 2008; Wu et al., 2012; Li S et al., 2015). In order to overcome the resistance mechanism caused by P-gp, recent researches have focused on the novel drug delivery system-lipid based nanoparticles (Susa et al., 2010; Dhule et al., 2012). Susa et al. have been proven that dextran nanoparticles loaded with DOX had a curative effect on MDR OS cell lines by increasing the amount of drug accumulation in the nucleus via P-gp independent pathway (Susa et al., 2009). Studies have shown the merit of curcumin (CUR) loaded nanocarriers for treatment of OS, including CUR-loaded self-assembled arginine-rich-RGD nanospheres, CUR liposomal nanoparticles, etc. (Dhule et al., 2014; Chang et al., 2015). In our present study, combined with the merit of combination therapy and lipid nanoparticles to obstacle MDR, we designed DOX plus CUR co-encapsulated lipid-coated polymeric nanoparticles (LPNs).

CUR, the constituent of *Curcuma longa* (turmeric), is known for its potent antineoplastic against a number of tumors, such as prostate, breast, colon cancer and OS (Chang

Address for correspondence: DongSheng Zhou, Department of Orthopaedics, Shandong Provincial Hospital Affiliated to Shandong University, 324 Jing Wu Road, Ji'nan 250021, P.R. China. Email: sdzhouds@163.com

et al., 2014; Troselj & Kujundzic, 2014). It influences a wide variety of cellular processes through the reshaping of many molecular targets. Tumor inhibitory activity is attributed to its inhibiting NF-κB and its up-regulation of p53 expression (the mechanism of anti-multidrug resistance); and its action on tumor necrosis factor (TNF-α), vascular endothelial growth factor (VEGF), cyclooxygenase, matrix metalloproteinase, etc. (Brennan & O'Neill, 1998; Collins et al., 2013; Chang et al., 2015). However, its poor aqueous solubility and low systemic bioavailability has become the obstacle to its clinical application.

While focusing on the combination therapy of DOX and CUR, we have explored further lipid based nanoparticles to enhance the solubility of CUR and the synergistic therapeutic efficacy. To overcome the rapid clearance effect of the reticuloendothelial system, polymeric nanoparticles were coated with lipid-polyethylene glycol (lipid-PEG) to form LPNs, thereby enhancing circulation lifetime and accessibility of nanoparticles to tumor. We hypothesized that DOX plus CUR co-encapsulated LPNs (DOX + CUR LPNs) could be an innovative strategy for the synergistic therapy of OS.

Materials and methods

Materials and reagents

Doxorubicin hydrochloride (DOX · HCl), CUR, cholesterol, triethylamine (TEA), 1,2-dilauroyl-sn-glycero-3-phos-phocholine (DLPC), dichloromethane (DCM) and (3-[4,5-dimehyl-2-thiazolyl]-2,5-diphenyl-2H-tetrazolium bromide (MTT) were purchased from Sigma-Aldrich Co., Ltd. (St Louis, MO). PEG_{2k}-DSPE was provided by Lipoid GmbH (Ludwigshafen, Germany). Poly (lactic-co-glycolic acid) (PLGA, molar ratio of D,L-lactic to glycolic acid, 50:50) was purchased from Ji'nan Daigang Biotechnology Co. Ltd. (Ji'nan, China). All other chemicals were of analytical grade or higher.

Cells and animals

Human OS cell lines (KHOS cells) were obtained from the American type culture collection (Manassas, VA). Cells were cultured in Dulbecco's Modified Eagle's Medium (DMEM) (Sigma, St. Louis, MO) supplemented with 10% fetal bovine serum (FBS) (Fisher Chemicals, Fairlawn, NJ) in a 5% CO_2 fully humidified atmosphere. BALB/c mice (6–8 weeks old, 18–22 g weight) were purchased from Medical Animal Test Center of Shandong Province (Ji'nan, China), and housed under standard laboratory conditions. The protocols were complied with the Animal Management Rules of the Ministry of Health of China.

Preparation of LPNs

DOX + CUR LPNs of mixed lipid monolayer shell and biodegradable polymer core were prepared as follows (Liu et al., 2010): DOX · HCl was stirred with TEA in DMSO overnight to obtain the DOX base (Miao et al., 2013). 50 mg of DOX, 100 mg of CUR and 500 mg of PLGA were dissolved in 10 mL of DCM to form the oil phase. Seven hundred milligrams of DLPC, 150 mg of cholesterol and 150 mg of PEG_{2k}-DSPE were dispersed in 20 mL of ultrapure water by sonication to form the aqueous phase. The oil phase was then poured into the water phase and the mixture was sonicated by probe ultrasonicator under ice bath. DCM was evaporated from the emulsion by magnetic stirring (600 rpm at room temperature). The suspension was centrifuged for 10 min (10 000 rpm at 4 °C) to collect the DOX + CUR LPNs.

DOX encapsulated LPNs (DOX LPNs), CUR encapsulated LPNs (CUR LPNs) and no drug encapsulated LPNs (LPNs) were prepared by the same method with the presence of one drug or no drug.

The obtained LPN suspensions were stored at 2–8 °C.

Particle morphology, size and zeta potential

The shape and surface morphology of the DOX + CUR LPNs were examined by transmission electronic microscopy (TEM) (Zhao et al., 2013). Samples were prepared by placing a drop of SLN suspension onto a copper grid and air-drying, followed by negative staining with one drop of 3% aqueous solution of sodium phosphotungstate for contrast enhancement. The air-dried samples were then directly examined under the TEM.

The mean particle size, polydispersity index (PDI) and zeta potential were analyzed by photon correlation spectroscopy (PCS), with a Zetasizer 3000 (Malvern Instruments, Malvern, UK) (Saini et al., 2015). The average particle size was expressed as volume mean diameter.

Drug encapsulation efficiency (DEE) and drug loading capacity (DLC)

The DEE and DLC of DOX or CUR were measured by UV–vis method (Ahangari et al., 2013). DOX + CUR LPNs, DOX LPNs or CUR LPNs were dissolved by adding a specific amount of ethanol and the concentration of DOX or CUR was determined with a UV–vis spectrophotometer. The selected wavelength for DOX and CUR measurement was 485 and 430 nm, respectively.

DEE were calculated as follows:

$$\text{DEE } (\%) = \frac{\text{Weight of(total drug} - \text{free drug)}}{\text{Weight of total drug} \times 100}.$$

DLC were calculated as follows:

$$\text{DLC } (\%) = \frac{\text{Weight of(total drug} - \text{free drug)}}{\text{Weight of total drug and lipid carriers} \times 100}.$$

Stability study

DOX + CUR LPNs, DOX LPNs or CUR LPNs were freshly prepared, isolated and re-suspended in 0.9% (w/v) physiological saline (Ye et al., 2015). Samples were incubated at 4 °C under agitation (100 rpm) and collected at different time points during a period of 35 days. The sizes of the drugs loaded LPNs were measured and summarized.

Stability study in the serum was determined in the presence of serum (Parajó et al., 2010). Samples were incubated in phosphate buffers (PBS) solution containing 10% (v/v) FBS at 37 °C for 12 h, separately. At scheduled times (0,

2, 4, 8 and 12 h), 1 mL of each sample was diluted with 2 mL THF and the mixture was bath sonicated for 5 min, followed by centrifugation at 10 000 rpm for 5 min. The variation trends of the sizes were measured and summarized.

In vitro drug release study

In vitro DOX or CUR released from drug loaded LPNs were measured by the dialysis method (Shao et al., 2015). One milliliter of DOX + CUR LPNs, DOX LPNs, CUR LPNs, DOX solution and CUR solution was placed in the dialysis bag separately. Then, the bag was incubated with 50 mL release medium (0.1% Tween-80 in PBS, pH 7.4). The medium (1 mL) was collected at predetermined time points and replaced with 50 mL of fresh medium. The concentrations of released DOX or CUR were determined by the UV–vis method in the above section.

In vitro cytotoxic study

The cytotoxicity was evaluated by MTT assay (Zaki, 2014). Briefly, KHOS cells were seeded in a 96-well plate at a density of 5×10^3 cells/well and allowed to adhere for 24 h prior to the assay. DOX + CUR LPNs, DOX LPNs, CUR LPNs, LPNs, DOX + CUR solution, DOX solution and CUR solution with varying concentrations were added to each well. The plates were then returned to the incubators. After 24 h, aliquots of MTT solution (20 mL) were added into each well after the designated period. The plates were then returned to the incubator. After 3 h of incubation, the growth medium in each well was removed and 150 mL of dimethylsulfoxide (DMSO) was added to each well to dissolve the internalized purple formazan crystals. An aliquot of 100 mL was taken from each well and transferred to a new 96-well plate. The plates were then assayed at the absorbance of 570 nm using a microplate reader (Model 680, BIO-RAD, Hercules, CA). Cells without the addition of MTT reagents were used as a blank to calibrate the spectrophotometer to zero absorbance.

Tissue distribution study

BALB/c mice were inoculating (s.c.) subcutaneously with 1×10^6 KHOS cells. The tumors were allowed to develop on the posterolateral side of the mice for one week prior to treatment (Gaudin et al., 2015). DOX + CUR LPNs and DOX + CUR solution were given into the mice by tail vein injection, separately. The *in vivo* organ distribution study of different samples was investigated in OS tumor-bearing BALB/c nude mice models at different time points during a period of five days after i.v. injection. At predetermined time intervals, mice were sacrificed and the tumor, heart, liver, spleen, lung and kidney of mice were collected. Tissues were initially weighed and homogenized with physiological saline to determine the amount of DOX or CUR in each tissue. The concentrations of released DOX or CUR were determined by the UV–vis method mentioned above.

In vivo anticancer evaluation

BALB/c mice were inoculating (s.c.) subcutaneously with 1×10^6 KHOS cells. The tumors were allowed to develop on the posterolateral side of the mice for one week prior to treatment. DOX + CUR LPNs (5 mg DOX/kg, 10 mg CUR/kg), DOX LPNs (10 mg DOX/kg), CUR LPNs (20 mg CUR/kg), LPNs, DOX + CUR solution (10 mg DOX/kg, 20 mg CUR/kg), DOX solution (10 mg DOX/kg) and CUR solution (20 mg CUR/kg) were administered intravenously every three days until three weeks. All efforts were made to minimize the suffering of the animals and to reduce the number of animals used and the mice were sacrificed by cervical dislocation. After the mice were sacrificed, the solid tumors were separated. The volumes of the solid tumor were measured with a digital caliper every three days and were calculated by the formula: Tumor volume $= (W^2 \times L)/2$, where W is the tumor measurement at the widest point and L the tumor dimension at the longest point. Tumor weights were measured and the tumor growth inhibition ratio (TGI) was calculated as follows: TGI (%) = (Weight of control − Weight of treated)/Weight of control × 100. The body weight was measured simultaneously as an indicator of systemic toxicity.

Statistical analysis

Results are reported as mean ± SD. Statistical significance was analyzed using Student's *t*-test. p Values less than 0.05 were considered as statistically significant.

Results

Preparation and characterization of LPNs

Figure 1 shows the shape and surface morphology of DOX + CUR LPNs. TEM images clearly delineated that the DOX + CUR LPNs had spheroidal shapes: they had gray coats on the darker spherical shaped particles. The size of DOX + CUR LPNs was about 100 nm according to the bars

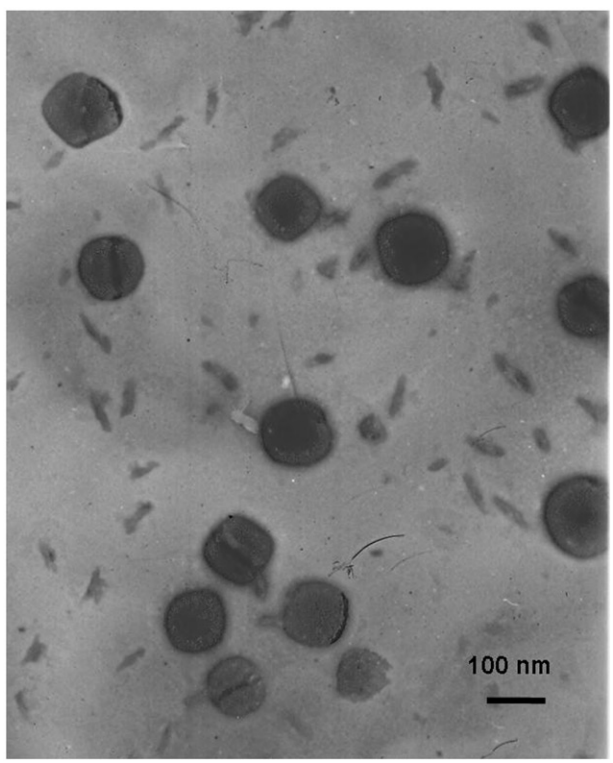

Figure 1. The shape and surface morphology of DOX + CUR LPNs.

in the images. In combination with the data of Table 2, the LPNs and LPNs loaded with one or two drugs exhibited particle size of around 100 nm. The zeta potential of DOX + CUR LPNs was −33.4 mV. No significant variations were observed in zeta potential of different samples.

The DEE of DOX loading in DOX + CUR LPNs and DOX LPNs was around 85%, the DEE of CUR was 80%. The DLC of DOX and CUR is also summarized in Table 1. Table 2 shows the time-dependent stability of the DOX + CUR LPNs, DOX LPNs and CUR LPNs. No significant change in particle size and DEE was observed up to 30 days, indicating that all the samples were stable in one month.

Stability study

Table 2 shows the time-dependent size changes of DOX + CUR LPNs, DOX LPNs or CUR LPNs. The average sizes of all LPNs studied were around 100 nm. No significant change in particle size was observed up to 35 days, indicating that DOX + CUR LPNs, DOX LPNs or CUR LPNs were stable in the physiological saline condition. The favorable stability of LPNs provides support for the loading and transporting of the DOX and/or CUR.

Changes in size in the presence of serum are described in Table 3. No significant change in particle size was observed in all samples in the FBS. Thus, DOX + CUR LPNs, DOX LPNs or CUR LPNs were considered very stable after incubation with serum and suggest that this formulation will not aggregate or disassemble after intravenous administration.

In vitro drug release

Figures 2 and 3 show the release curve of DOX and CUR from the LPNs and solutions. The drugs release from the LPNs had a fast release of drugs during the first 12 h, followed by a sustained release in the subsequent time until 48 h. The releases of drugs from solutions were fast and complete with the first 2 h. The *in vitro* release profiles show that drugs loaded LPNs have the capacity to release DOX and CUR at a sustained rate over 48 h.

In vitro cytotoxicity

To test the *in vitro* anti-OS efficacy of various kinds of samples, we evaluated the performance of DOX + CUR LPNs, DOX LPNs, CUR LPNs, LPNs, DOX + CUR solution, DOX solution and CUR solution in KHOS cells. Figure 4 shows the viabilities of cancer cells evaluated by MTT assay. The results illustrated that over the studied drug concentrations, the cytotoxicity of the dual drugs loaded LPNs was higher than single drug loaded LPNs ($p < 0.05$); cytotoxicity of the drug loaded LPNs was higher than free drug solutions ($p < 0.05$). The IC_{50} values are summarized in Table 4. The IC_{50} of DOX + CUR LPNs was the lowest (0.6 μM). The IC_{50} values of drug loaded LPNs were many folds dose advantage over the free drug solutions.

In vivo tissue distribution

In vivo DOX tissue distribution results of DOX + CUR LPNs and DOX + CUR solution are shown in Figures 5 and 6. CUR tissue distribution results of DOX + CUR LPNs and DOX + CUR solution are shown in Figures 7 and 8. Figures 6 and 8 illustrate that the drug solution mainly distributes in heart and kidney. DOX and CUR distribution of DOX + CUR LPNs was higher in the tumor tissue compared with the other tissues (Figures 5 and 7). The higher concentration in the tumor tissue remained relatively stable at all time points until 48 h after injection, indicating the sustained-release behavior of the DOX + CUR LPNs.

In vivo anticancer evaluation

The *in vivo* antitumor efficiency was evaluated in the KHOS cells bearing OS mice model. As illustrated in Figure 9, most obvious tumor regressions were clearly observed in the DOX + CUR LPNs group, the tumor growth was prominently delayed, which attained about 182 mm^3, whereas in saline-

Table 2. Time-dependent size changes of LPNs.

Time (days)	DOX LPNs	CUR LPNs	DOX + CUR LPNs
1	100.2 ± 3.5	99.8 ± 3.7	101.9 ± 4.8
2	101.1 ± 2.6	100.8 ± 3.2	100.4 ± 2.9
3	103.3 ± 3.9	101.6 ± 2.9	99.6 ± 4.1
4	101.5 ± 3.7	103.7 ± 4.8	102.6 ± 3.4
5	103.1 ± 3.9	101.4 ± 3.2	100.4 ± 4.2
10	101.7 ± 3.1	102.3 ± 2.9	99.1 ± 4.6
15	99.3 ± 5.1	101.8 ± 3.4	102.6 ± 3.7
20	100.4 ± 4.2	102.7 ± 4.6	101.8 ± 3.2
25	101.1 ± 2.9	99.8 ± 4.4	103.1 ± 2.7
35	102.1 ± 3.6	101.4 ± 4.2	101.9 ± 3.8

Table 3. Size changes of LPNs in serum.

Time (h)	DOX LPNs	CUR LPNs	DOX + CUR LPNs
0	102.1 ± 3.7	101.3 ± 4.1	100.5 ± 4.4
2	103.3 ± 3.1	100.2 ± 3.9	101.1 ± 4.9
4	102.1 ± 3.3	102.1 ± 3.6	102.3 ± 3.7
8	102.7 ± 4.1	101.9 ± 4.3	102.9 ± 4.1
12	102.3 ± 4.3	102.3 ± 3.8	101.8 ± 4.6

Table 1. Preparation and characterization of LPNs.

Formulations	LPNs	DOX LPNs	CUR LPNs	DOX + CUR LPNs
Particle size (nm)	96.7 ± 2.6	100.2 ± 3.5	99.8 ± 3.7	101.9 ± 4.8
PDI	0.13 ± 0.03	0.17 ± 0.04	0.19 ± 0.05	0.21 ± 0.06
Zeta potential (mV)	−31.9 ± 3.4	−30.5 ± 3.6	−32.7 ± 3.1	−33.4 ± 4.1
DEE of DOX (%)	N/A	85.6 ± 3.9	N/A	84.9 ± 2.9
DEE of CUR (%)	N/A	N/A	80.6 ± 2.8	81.6 ± 3.3
DLC of DOX (%)	N/A	13.2 ± 1.2	N/A	9.1 ± 0.9
DLC of CUR (%)	N/A	N/A	10.6 ± 1.4	8.3 ± 1.0

treated group, tumor volume grew rapidly to 973 mm^3 on 21-day post-treatment. The TGI of OS mice treated with the DOX + CUR LPNs was 81.3%, which was significantly higher than that treated with other samples (Table 5). The obvious emaciation could be observed in the free drug solution groups, while the LPN groups did not cause significant difference in body weight loss (Figure 10). During the treatment, reduction in food intake, energy sag and inactive in moving were also observed in the free drug solution groups but not in other groups.

Discussion

DOX + CUR LPNs had spheroidal shapes and there are gray coats on the darker spherical shaped particles (Figure 1). The darker parts in the middle are the drugs loaded polymeric core care and the gray coats are the lipid shell. The size of DOX + CUR LPNs was about 100 nm (Table 1). The size of LPNs loaded with one or two drugs had no significant variation ($p > 0.05$). This could be the evidence that loading of drugs would not enlarge the particle size of LPNs. Nano-sized particles can prolong the blood circulation time and mediated the tumor targeting of the drugs they carried (Ganta et al., 2015). The 100 nm size of DOX + CUR LPNs is expected to increase the cellular uptake of delivery systems, and improved bioavailability of both DOX and CUR. The zeta potential of DOX + CUR LPNs was −33.4 mV. No obvious variations were observed in zeta potential of different samples ($p > 0.05$). The DEE of both two drug loadings in all kinds of LPNs showed no significant variations ($p > 0.05$). These results suggest that the loading of two drugs did not affect the encapsulation efficiency of each other (Li Y et al., 2015). This phenomenon may be due to the stable ability of the LPNs. DOX + CUR LPNs, DOX LPNs and CUR LPNs show no significant change in particle size and DEE in a period of 30

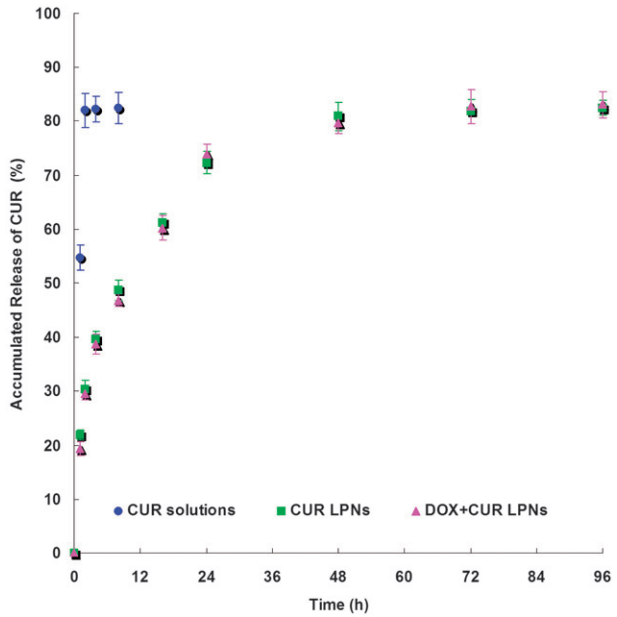

Figure 3. The release curve of CUR from the LPNs and solutions.

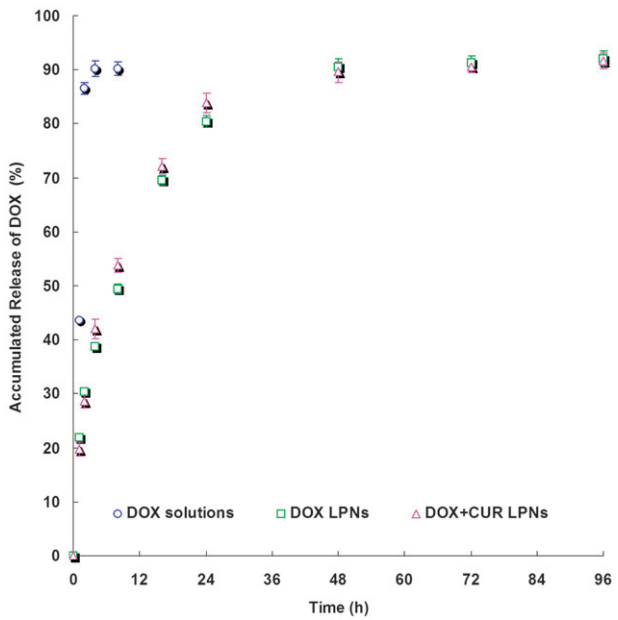

Figure 2. The release curve of DOX from the LPNs and solutions.

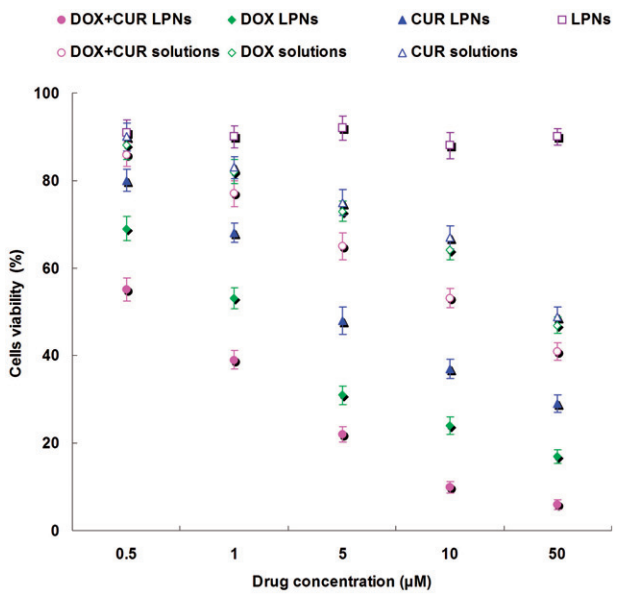

Figure 4. The viabilities of KHOS cells evaluated by MTT assay.

Table 4. The IC_{50} values.

Formulations	DOX solution	CUR solution	DOX + CUR solution	DOX LPNs	CUR LPNs	DOX + CUR LPNs
IC_{50} of DOX (μM)	46.5 ± 3.1	N/A	11.7 ± 1.8	2.1 ± 0.6	N/A	0.6 ± 0.1
IC_{50} of CUR (μM)	N/A	49.3 ± 3.9	11.7 ± 1.8	N/A	4.6 ± 0.9	0.6 ± 0.1

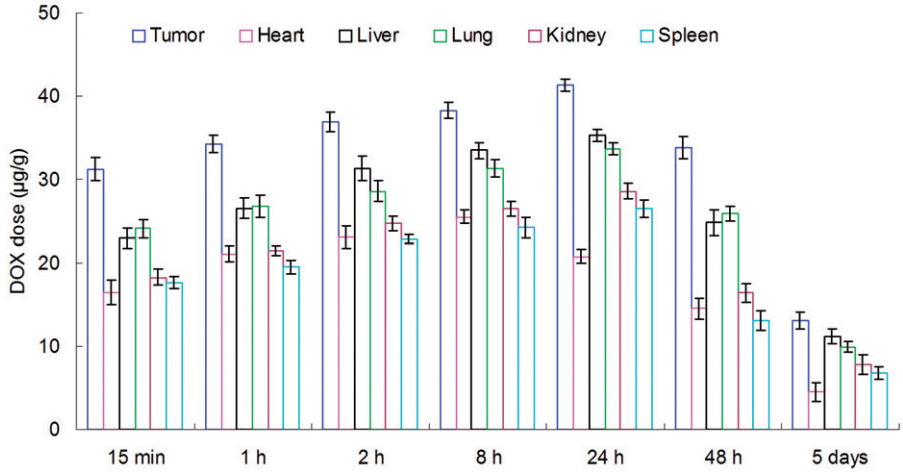

Figure 5. *In vivo* DOX tissue distribution results of DOX + CUR LPNs.

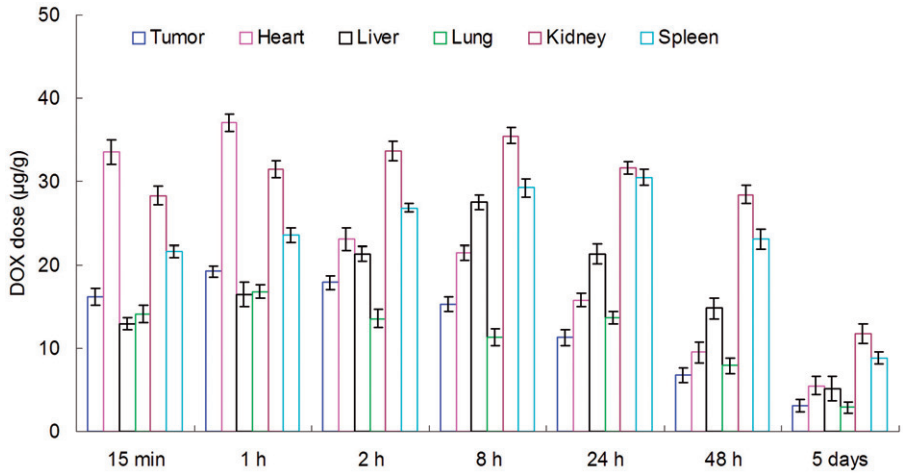

Figure 6. *In vivo* DOX tissue distribution results of DOX + CUR solution.

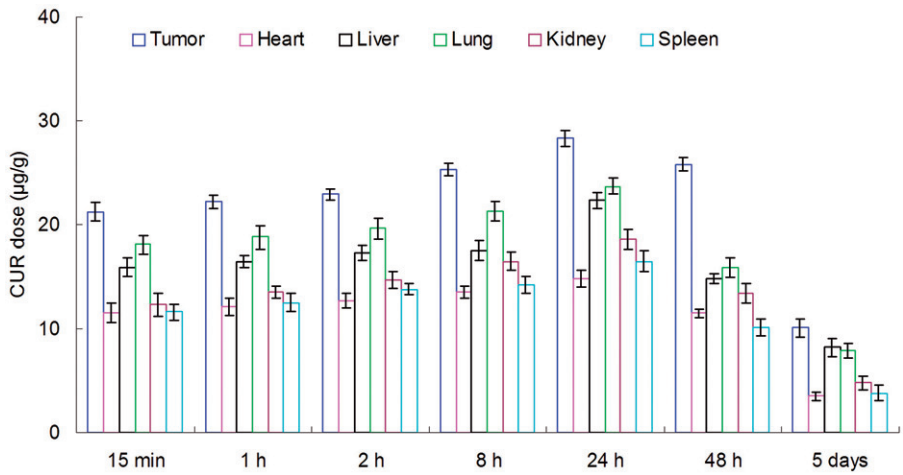

Figure 7. *In vivo* CUR tissue distribution results of DOX + CUR LPNs.

days and in the presence of serum (Tables 2 and 3, $p > 0.05$), indicating that all the samples were relatively stable (Ye et al., 2015).

The drug releases from the LPNs had a fast release of drugs during the first 12 h, followed by a sustained release in the subsequent time until 48 h (Figure 2). The releases of drugs from solutions were fast and complete with the first 2 h (Figure 3). The releases of DOX from LPNs were faster than that of CUR. The drug release from nanoparticles generally takes place by several mechanisms, including surface and bulk erosion, disintegration, diffusion, or desorption (Rahman et al., 2013). This sustained release of drug from nanoparticles is due to homogenous entrapment of the drug. The drugs enriched polymer core can

Figure 8. *In vivo* CUR tissue distribution results of DOX + CUR solution.

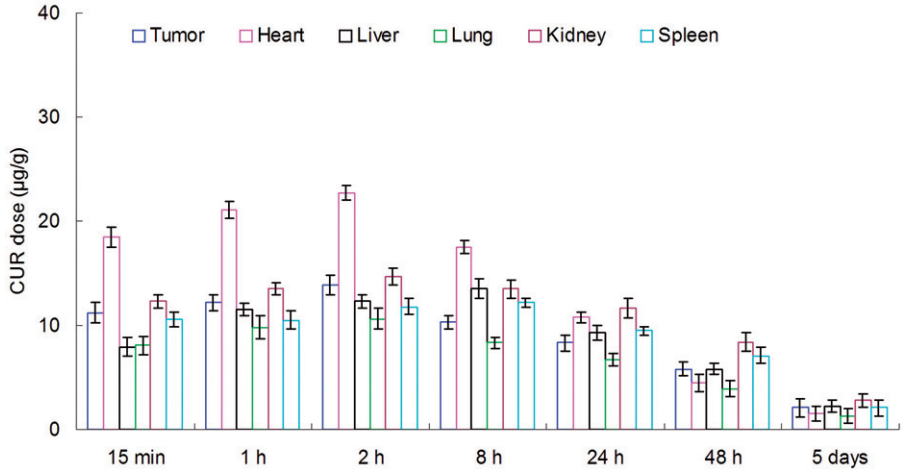

Figure 9. *In vivo* antitumor efficiency in the KHOS cells bearing OS mice model.

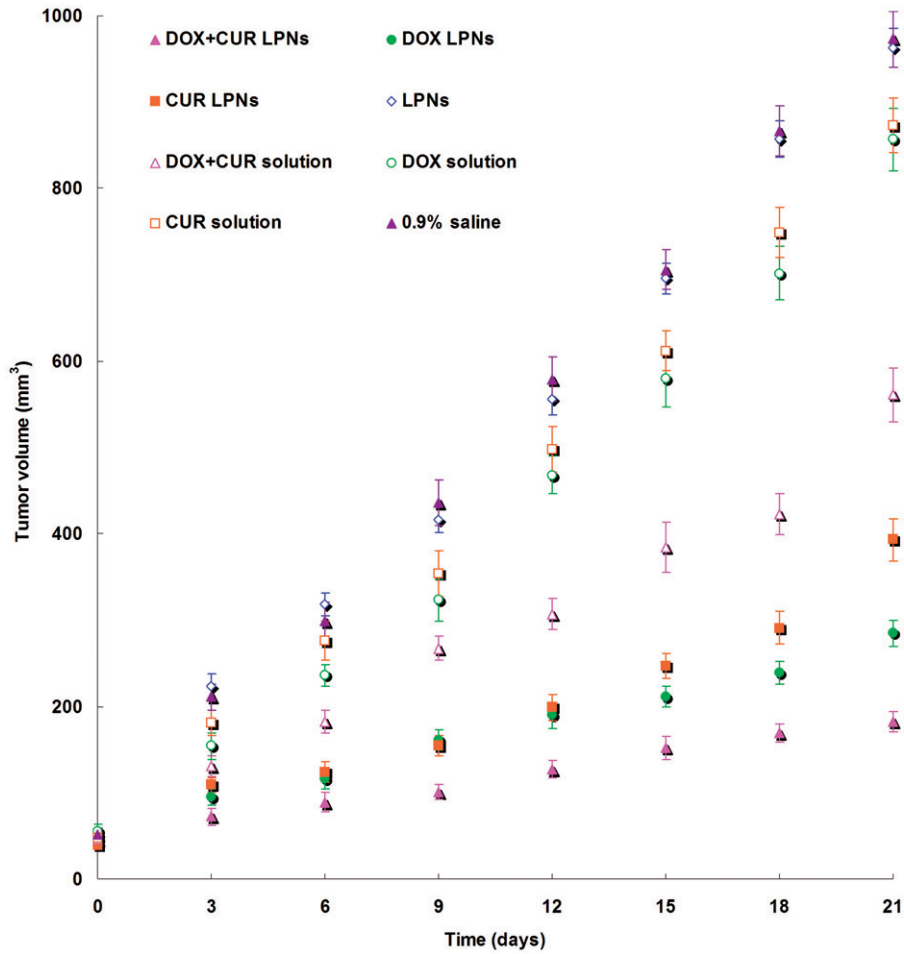

Table 5. Tumor growth inhibition ratio (TGI).

Formulations	DOX solution	CUR solution	DOX + CUR solution	DOX LPNs	CUR LPNs	DOX + CUR LPNs
TGI (%)	10.3	11.9	42.3	59.6	70.7	81.3

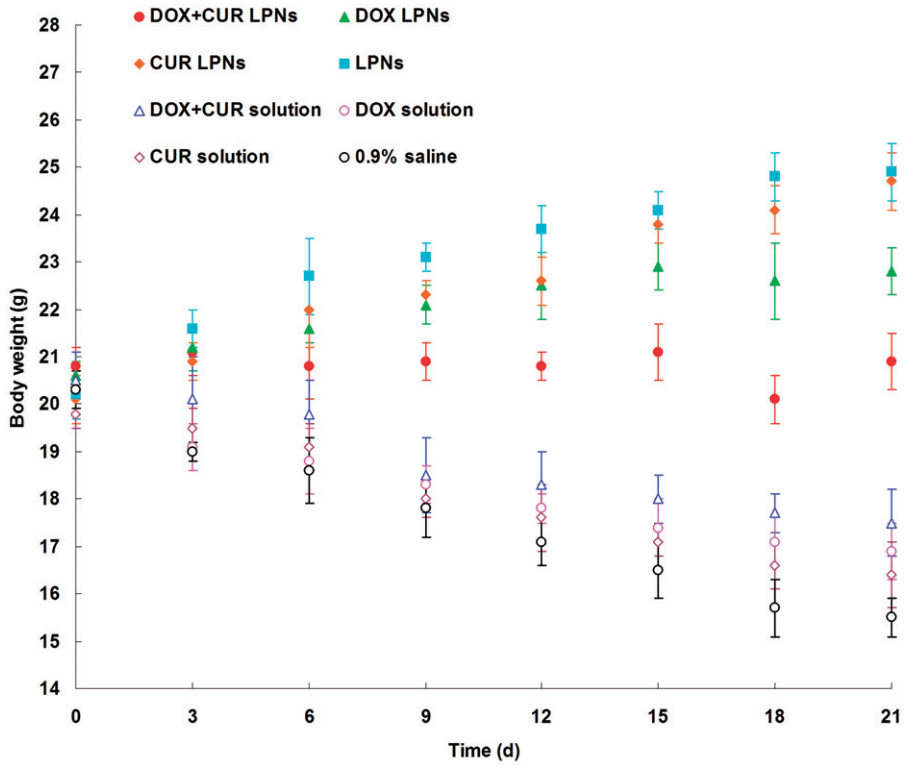

Figure 10. Body weight changes in the KHOS cells bearing OS mice model.

slow down the release of the drugs. Also the surface coating of lipids could slow the release of drug from LPNs. The *in vitro* release profiles show that drugs loaded LPNs have the capacity to release DOX and CUR at a sustained rate over 48 h, thus let the drugs contentiously develop the therapeutic effect.

In vitro anti-OS efficacy of various kinds of samples was evaluated in KHOS cells by MTT assay (Figure 4). The results illustrated that over the studied drug concentrations, the cytotoxicity of the dual drugs loaded LPNs was higher than single drug loaded LPNs ($p < 0.05$); cytotoxicity of the drug loaded LPNs was higher than free drug solutions ($p < 0.05$). The IC_{50} of DOX + CUR LPNs was the lowest among all the samples tested. The IC_{50} values of drug loaded LPNs were many folds dose advantage over the free drug solutions. These results could be explained as follows: Firstly, the construction of LPN systems could improve the delivery of drugs thus gain better efficiency than free drugs; Secondly, the combined antitumor effect of the dual drugs loaded LPNs performed better than the single drug loaded ones (Li Y et al., 2015).

In vivo DOX and CUR distribution of DOX + CUR solution was mainly in heart and kidney (Figures 6 and 8). This could lead to systemic toxicity. DOX and CUR distribution of DOX + CUR LPNs was higher in the tumor tissue compared with the other tissues (Figures 5 and 7). This could decrease the side effects during the tumor therapy. Solid tumors have leakage microvasculatures (Dubey et al., 2012). Smaller particle size was favorable for passive targeting to the tumor owing to the ''enhanced permeability and retention'' (EPR) effects which resulted in the efficient accumulation in tumor of the LPNs. Also the higher distribution percent in tumor of LPNs might be due to the prolonged blood circulation time.

In vivo antitumor efficiency was evaluated in the KHOS cells bearing OS mice model. Although DOX and CUR are among the most effective anticancer agents against OS, it is associated with various systemic side effects, such as nephrotoxicity, myelosuppression, neurotoxicity, nausea and emesis (Wang et al., 2013). LPNs formulations in this study were used to overcome these side effects and achieve high anticancer efficiency. As illustrated in Figure 9, most obvious tumor regressions were clearly observed in the DOX + CUR LPNs group, the tumor growth was prominently delayed. The TGI of OS mice treated with the DOX + CUR LPNs was the highest (Table 4). The obviously emaciation could be observed in the free drug solutions groups, while the LPN groups did not cause significant difference in body weight loss (Figure 10). During the treatment, reduction in food intake, energy sag and inactive in moving were also observed in the free drug solution groups but not in other groups. The results suggested the best antitumor effect of DOX + CUR LPNs due to the synergetic effect of the two drugs and the least systemic toxic side effect of the LPNs formulations for the OS treatment.

Conclusions

DOX + CUR LPNs were prepared and used for the delivery of DOX and COU to the OS cells to inhibit the cell viability. Furthermore, the DOX + CUR LPNs effectively improve anticancer efficiency for OS bearing mice without causing obvious toxicity *in vivo*. These results demonstrate that the dual drugs co-encapsulated LPNs may have potential to be

used as promising drug delivery system for the treatment of OS.

Declaration of interest

The authors report no conflicts of interest. The authors alone are responsible for the content and writing of this article.

References

Ahangari A, Salouti M, Heidari Z, et al. (2013). Development of gentamicin-gold nanospheres for antimicrobial drug delivery to Staphylococcal infected foci. Drug Deliv 20:34–9.

Brennan P, O'Neill LA. (1998). Inhibition of nuclear factor kappaB by direct modification in whole cells-mechanism of action of nordihydroguaiaritic acid, curcumin and thiol modifiers. Biochem Pharmacol 55:965–73.

Chang R, Sun L, Webster TJ. (2014). Short communication: selective cytotoxicity of curcumin on osteosarcoma cells compared to healthy osteoblasts. Int J Nanomed 9:461–5.

Chang R, Sun L, Webster TJ. (2015). Selective inhibition of MG-63 osteosarcoma cell proliferation induced by curcumin-loaded self-assembled arginine-rich-RGD nanospheres. Int J Nanomed 10: 3351–65.

Collins HM, Abdelghany MK, Messmer M, et al. (2013). Differential effects of garcinol and curcumin on histone and p53 modifications in tumour cells. BMC Cancer 13:37.

Desandes E. (2007). Survival from adolescent cancer. Cancer Treat Rev 33:609–15.

Dhule SS, Penfornis P, Frazier T, et al. (2012). Curcumin-loaded γ-cyclodextrin liposomal nanoparticles as delivery vehicles for osteosarcoma. Nanomedicine 8:440–51.

Dhule SS, Penfornis P, He J, et al. (2014). The combined effect of encapsulating curcumin and C6 ceramide in liposomal nanoparticles against osteosarcoma. Mol Pharm 11:417–27.

Dubey N, Varshney R, Shukla J, et al. (2012). Synthesis and evaluation of biodegradable PCL/PEG nanoparticles for neuroendocrine tumor targeted delivery of somatostatin analog. Drug Deliv 19:132–42.

Gao X, Wang B, Wei X, et al. (2013). Preparation, characterization and application of star-shaped PCL/PEG micelles for the delivery of doxorubicin in the treatment of colon cancer. Int J Nanomed 8: 971–82.

Ganta S, Singh A, Rawal Y, et al. (2015). Formulation development of a novel targeted theranostic nanoemulsion of docetaxel to overcome multidrug resistance in ovarian cancer. Drug Deliv 21:1–13.

Gaudin A, Lepetre-Mouelhi S, Mougin J, et al. (2015). Pharmacokinetics, biodistribution and metabolism of squalenoyl adenosine nanoparticles in mice using dual radio-labeling and radio-HPLC analysis. J Control Release 212:50–8.

Li S, Sun W, Wang H, et al. (2015). Research progress on the multidrug resistance mechanisms of osteosarcoma chemotherapy and reversal. Tumour Biol 36:1329–38.

Li Y, Su T, Zhang Y, et al. (2015). Liposomal co-delivery of daptomycin and clarithromycin at an optimized ratio for treatment of methicillin-resistant *Staphylococcus aureus* infection. Drug Deliv 22:627–37.

Liu Y, Li K, Pan J, et al. (2010). Folic acid conjugated nanoparticles of mixed lipid monolayer shell and biodegradable polymer core for targeted delivery of Docetaxel. Biomaterials 31:330–8.

Longhi A, Errani C, De Paolis M, et al. (2006). Primary bone osteosarcoma in the pediatric age: state of the art. Cancer Treat Rev 32:423–36.

Miao J, Du YZ, Yuan H, et al. (2013). Drug resistance reversal activity of anticancer drug loaded solid lipid nanoparticles in multi-drug resistant cancer cells. Colloids Surf B Biointerfaces 110:74–80.

Nedelcu T, Kubista B, Koller A, et al. (2008). Livin and Bcl-2 expression in high-grade osteosarcoma. J Cancer Res Clin Oncol 134: 237–44.

Parajó Y, D'Angelo I, Welle A, et al. (2010). Hyaluronic acid/chitosan nanoparticles as delivery vehicles for VEGF and PDGF-BB. Drug Deliv 17:596–604.

Rajkumar T, Yamuna M. (2008). Multiple pathways are involved in drug resistance to doxorubicin in an osteosarcoma cell line. Anticancer Drugs 19:257–65.

Rahman HS, Rasedee A, How CW, et al. (2013). Zerumbone-loaded nanostructured lipid carriers: preparation, characterization, and antileukemic effect. Int J Nanomed 8:2769–81.

Saini D, Fazil M, Ali MM, et al. (2015). Formulation, development and optimization of raloxifene-loaded chitosan nanoparticles for treatment of osteoporosis. Drug Deliv 22:823–36.

Schwartz CL, Gorlick R, Teot L, et al. (2007). Multiple drug resistance in osteogenic sarcoma: INT0133 from the Children's Oncology Group. J Clin Oncol 25:2057–62.

Siegel R, Naishadham D, Jemal A. (2013). Cancer statistics, 2013. CA Cancer J Clin 63:11–30.

Shao Z, Shao J, Tan B, et al. (2015). Targeted lung cancer therapy: preparation and optimization of transferrin-decorated nanostructured lipid carriers as novel nanomedicine for co-delivery of anticancer drugs and DNA. Int J Nanomed 10:1223–33.

Susa M, Iyer AK, Ryu K, et al. (2009). Doxorubicin loaded polymeric nanoparticulate delivery system to overcome drug resistance in osteosarcoma. BMC Cancer 9:399.

Susa M, Iyer AK, Ryu K, et al. (2010). Inhibition of ABCB1 (MDR1) expression by an siRNA nanoparticulate delivery system to overcome drug resistance in osteosarcoma. PLoS One 5:e10764.

Troselj KG, Kujundzic RN. (2014). Curcumin in combined cancer therapy. Curr Pharm Des 20:6682–96.

Wang Y, Liu P, Qiu L, et al. (2013). Toxicity and therapy of cisplatin-loaded EGF modified mPEG-PLGA-PLL nanoparticles for SKOV3 cancer in mice. Biomaterials 34:4068–77.

Wu X, Cai ZD, Lou LM, et al. (2012). Expressions of p53, c-MYC, BCL-2 and apoptotic index in human osteosarcoma and their correlations with prognosis of patients. Cancer Epidemiol 36: 212–16.

Ye YJ, Wang Y, Lou KY, et al. (2015). The preparation, characterization, and pharmacokinetic studies of chitosan nanoparticles loaded with paclitaxel/dimethyl-β-cyclodextrin inclusion complexes. Int J Nanomed 10:4309–19.

Zaki NM. (2014). Augmented cytotoxicity of hydroxycamptothecin-loaded nanoparticles in lung and colon cancer cells by chemosensitizing pharmaceutical excipients. Drug Deliv 21:265–75.

Zhao M, Li A, Chang J, et al. (2013). Develop a novel super-paramagnetic nano-carrier for drug delivery to brain glioma. Drug Deliv 20:95–101.